

# Molecular simulation and experimental studies of the miscibility of PLA/PLA<sub>x</sub>-PEG<sub>y</sub>-PLA<sub>x</sub> blends

Adisak Takhulee<sup>1</sup> · Yoshiaki Takahashi<sup>2</sup> · Visit Vao-soongnern<sup>1</sup>

Received: 1 May 2017 / Accepted: 28 September 2017 / Published online: 4 October 2017  
© Springer Science+Business Media B.V. 2017

**Abstract** To design a more efficient plasticizer for PLA based on PEG derivative, the miscibility enhancement of PLA/PLA<sub>x</sub>-PEG<sub>y</sub>-PLA<sub>x</sub> blends were investigated by both atomistic and mesoscale simulations. Flory-Huggins interaction parameters ( $\chi_{ij}$ ) of PLA<sub>x</sub>-PEG<sub>y</sub>-PLA<sub>x</sub> blends, with PLA block fractions = 0.1–0.5, were calculated using molecular dynamic (MD) simulation to determine the miscibility of PLA/PLA<sub>x</sub>-PEG<sub>y</sub>-PLA<sub>x</sub> blends and compared with PLA/PEG blends (Takhulee et al. J Polym Res 24:8, 2017). Based on the calculated  $\chi_{ij}$  and radial distribution functions, PLA/PLA<sub>x</sub>-PEG<sub>y</sub>-PLA<sub>x</sub> showed better miscibility compared to PLA/PEG. The values of  $\chi_{ij}$  for PLA/PLA<sub>x</sub>-PEG<sub>y</sub>-PLA<sub>x</sub> blends are always lower than those for PLA/PEG blends at the same PEG composition. For PLA/PLA<sub>x</sub>-PEG<sub>y</sub>-PLA<sub>x</sub> blends,  $\chi_{ij}$  increased as a function of PLA block fractions. Mesoscale properties of PLA/PLA<sub>x</sub>-PEG<sub>y</sub>-PLA<sub>x</sub> blends were then determined using dissipative particle dynamic (DPD) simulation. Smaller PEG domain in PLA/PLA<sub>x</sub>-PEG<sub>y</sub>-PLA<sub>x</sub> blends was observed, compared to that in PLA/PEG blend. Miscibility behavior of PLA/PLA<sub>x</sub>-PEG<sub>y</sub>-PLA<sub>x</sub> blends was investigated by experiments at selected conditions based on the simulation results. By differential scanning calorimetry measurements, acceleration of the crystallization of PLA matrix by blending PLA<sub>x</sub>-PEG<sub>y</sub>-PLA<sub>x</sub> was observed. Although PLA/PEG 70/30 (wt/wt)

blend was phase separated when slowly cooled from the melt, due to the crystallization of PEG component, this phenomenon was not observed in PLA/PLA<sub>x</sub>-PEG<sub>y</sub>-PLA<sub>x</sub> blends. The melting temperature ( $T_m$ ) depression of PLA/PLA<sub>x</sub>-PEG<sub>y</sub>-PLA<sub>x</sub> blends was also more pronounced. From dynamic mechanical analysis, the storage ( $G'$ ) and loss moduli ( $G''$ ) curves in terminal region were determined. The slope of  $G'$  curves for PLA/PEG 75/25 and 70/30 (wt/wt) was less than 2 while this deviation was found only at 70/30 (wt/wt) for PLA/PLA<sub>x</sub>-PEG<sub>y</sub>-PLA<sub>x</sub>. These results indicate that PLA<sub>x</sub>-PEG<sub>y</sub>-PLA<sub>x</sub> is better miscible with PLA.

**Keywords** PLA · Triblock copolymer · Blends · Molecular simulation

## Introduction

Poly(lactic acid) (PLA) is a biodegradable polymer which has attracted considerable research efforts in the variety applications. However, because of its inherent brittle nature and low thermal stability, PLA needs to be modified to be suitable for use in various applications where mechanical properties are important. There have been a considerable number of studies on toughening PLA with the goal of balancing and increasing tensile strength, impact strength and modulus while retaining the biocompatible and biodegradable nature [1–6].

One of the most efficient methods for toughening PLA is plasticization with low molecular weight polymers such as polyethylene glycol (PEG) which has been intensively studied for using as the plasticizer because of its low cost, biocompatible, and non-toxicity. However, the promising mechanical properties of PLA/PEG blends disappear with time due to the slow phase separation and crystallization of PEG component from

✉ Visit Vao-soongnern  
visit@sut.ac.th

<sup>1</sup> Laboratory of Computational and Applied Polymer Science, School of Chemistry, Institute of Science, Suranaree University of Technology, Nakhon Ratchasima 30000, Thailand

<sup>2</sup> Evaluation Office of Materials Properties, Institute for Materials Chemistry and Engineering, Kyushu University, Kasuga, Fukuoka 816-8580, Japan

homogeneous blends [7, 8]. To minimize the migration and phase separation of plasticizers in the blend, usage of block copolymers, for which one part of block segment is identical or miscible within polymer matrix and another part is a chemical acting as plasticizer, have been proposed. The end block of copolymer has several molecular effects. First, the interface tension between the phases is lowered, which reduces the driving force for the phase separation. Secondly, the presence of the end block of copolymer at the interface reduces the tendency of the domains to coalesce. [9, 10]. There have been some past experimental investigation regarding the use of block copolymers as plasticizer [11–13].

It is widely accepted that phase behavior of block copolymer/homopolymer blends is quite complicated even homopolymer and one component of block is the same polymer. It is quite difficult to find optimum condition for good plasticizer by experimental study alone. Molecular simulation gains acceptance as a reliable technique to analyze the microscopic and mesoscopic insights into the phase morphology and interfacial behaviors of multiphase polymer systems. Molecular simulation provides a bridge between model and experiments, as the method is using mathematical models to perform an analysis by computers. For example, several MD simulation techniques were applied to calculate polymer-polymer interactions in order to predict the miscibility of polymer blends [14, 15]. However, the broad range of time scales and underlying structures prohibits the fully atomistic simulation method that captures all of these processes. The coarse-graining model or mesoscale method has been successful in extending of the scope. In this model about four to five of carbon atoms in a polymer chain are grouped into a single bead and thus many states can be easily generated and equilibrated. One example is the dissipative particle dynamics (DPD), a mesoscale simulation technique developed to model Newtonian and non-Newtonian fluids [16]. It is capable to investigate the phase morphology and interface properties of multiphase systems.

This work is the second report following our previous publication on simulation of PLA/PEG system supported by experiments at selected conditions [17]. The organization of this paper is as follows: First, MD and DPD simulations are employed to predict the miscibility and morphology of  $\text{PLA}_x\text{-PEG}_y\text{-PLA}_x$  systems. Then, preparation and characterization of  $\text{PLA}_x\text{-PEG}_y\text{-PLA}_x$  block copolymer and PLA/ $\text{PLA}_x\text{-PEG}_y\text{-PLA}_x$  blends are reported. The characteristics of  $\text{PLA}_x\text{-PEG}_y\text{-PLA}_x$  triblock copolymer were evaluated by NMR spectroscopy and gel permeation chromatography (GPC). Thermal and rheological properties of PLA/PEG and PLA/ $\text{PLA}_x\text{-PEG}_y\text{-PLA}_x$  blends are then investigated to evaluate the miscibility of the blends.

## Simulation and experimental methods

### Molecular dynamic simulation

Miscibility of PLA/ $\text{PLA}_x\text{-PEG}_y\text{-PLA}_x$  blends were investigated using Discover Molecular Dynamic Simulation module (Materials Studio Version 4.0, Accelrys). All polymer chains were built based on the rotational isomeric state (RIS) model [18] to describe the conformational characteristics of polymer chains. The cubic simulation boxes were then constructed using the Amorphous Cell module based on the packing technique of Theodorou and Suter [19] and Meirovitch scanning method [20]. The polymer density in a simulation box corresponds to the bulk density of each polymer, i.e., PLA and PEG are 1.206 and 1.127 g/cm<sup>3</sup>, respectively. To avoid long simulation time, the appropriate chain lengths for PLA and PEG were determined by finding the solubility parameter ( $\delta$ ) as a function of chain length. The optimized length for PLA and PEG were 30 and 50 of repeating units, respectively [21, 22]. It should be noted that these chain lengths are not the ones used in the Experimental Section but long enough for fully atomistic MD simulation to obtain reliable results for miscibility prediction. In this respect,  $\text{PLA}_3\text{-PEG}_{50}\text{-PLA}_3$ ,  $\text{PLA}_{11}\text{-PEG}_{50}\text{-PLA}_{11}$  and  $\text{PLA}_{25}\text{-PEG}_{50}\text{-PLA}_{25}$  (denoted as BL1, BL3 and BL5, respectively) corresponding to the PLA block fraction ( $f_{\text{PLA}}$ ) of 0.107, 0.306 and 0.500 were selected to explore the miscibility behavior with PLA. MD simulated systems of PLA/PEG and PLA/ $\text{PLA}_x\text{-PEG}_y\text{-PLA}_x$  blends are presented in Table 1.

After amorphous bulk polymer structure was constructed, energy minimization was subsequently carried out to eliminate the local non-equilibrium structures with the convergence threshold of 0.001 kcal/mol Å. Then NPT-MD was performed at 500 K and 1 bar for 2 ns to ensure that polymers are in the molten (amorphous) state (melting temperatures of PLA, PEG and  $\text{PLA}_x\text{-PEG}_y\text{-PLA}_x$  are 433–453 K, 333 K and 333–453 K, respectively). In order to further relax local hot-spots and to allow the system to achieve equilibrium, the structures were subjected to 10-circle thermal annealing from 300 to 1000 K and then back to 300 K with 50 K intervals. At each temperature, 100 ps NPT-MD simulation was performed at 1 bar with the time step of 1 fs. After this 10-circle annealing, then 2 ns NVT-MD simulation was carried out. At the last stage, 1 ns NVT-MD simulation was performed to collect data and trajectories were saved every 1 ps and used for analysis. In this work, the COMPASS (Condensed phase Optimized Molecular Potentials for Atomistic Simulation Studies) force field which is the first ab initio force field used for modeling interatomic interactions and specially optimized to provide accurate condensed phase equation of state and cohesive properties for molecules containing a wide range of functional groups was used [23].

**Table 1** Systems of MD Simulation of PLA/PEG and PLA/PLA<sub>x</sub>-PEG<sub>y</sub>-PLA<sub>x</sub> blends

System	LA units	EG units	Block units*	Number of chains	Composition (wt% PLA)	Density (g/cm <sup>3</sup> )
PLA	30	–	–	1 PLA	100	1.206
PEG	–	50	–	1 PEG	–	1.127
PLA/PEG 50/50	30	50	–	1PLA/1PEG	50	1.167
PLA/BL1 50/50	30	–	56	5PLA/5BL1	50	1.190
PLA/BL3 50/50	30	–	72	5PLA/5BL3	50	1.198
PLA/BL5 50/50	30	–	100	5PLA/5BL5	50	1.206

\* Atomistic model of PLA<sub>3</sub>-PEG<sub>50</sub>-PLA<sub>3</sub>, PLA<sub>11</sub>-PEG<sub>50</sub>-PLA<sub>11</sub> and PLA<sub>25</sub>-PEG<sub>50</sub>-PLA<sub>25</sub> are denoted as BL1, BL3 and BL5 for  $f_{PLA}$  = 0.107, 0.306 and 0.500, respectively

**Dissipative particle dynamics**

Dissipative Particle Dynamics (DPD) [24], is a mesoscale method for simulation of coarse-grained systems over a longer length and time scales than MD. In DPD simulation, several atoms or repeating units are grouped together into a single bead. The polymer chains in DPD can be considered to consist of number of beads ( $N_{DPD}$ ) calculated by:

$$N_{DPD} = \frac{M_p}{M_m C_n} = \frac{N}{C_n} \tag{1}$$

where  $N_{DPD}$  is number of beads,  $M_p$  is polymer molar mass,  $M_m$  is molar mass of repeating units,  $C_n$  is the characteristic ratio and  $N$  is number of repeating units.  $C_n$  can be calculated using Synthia module in Materials Studio software. (3.40 and 4.98 for PLA and PEG, respectively).

The force acting on each bead is a sum of three pairwise contributions, conservative force ( $f^C$ ), dissipative force ( $f^D$ ) and random force ( $f^R$ ):

$$f_i = \sum_{j \neq i} (f_{ij}^C + f_{ij}^D + f_{ij}^R) \tag{2}$$

where the sum runs over all other particles within a certain cutoff radius ( $r_c$ ). As this is the only length-scale in the system, we use the cutoff radius as our unit of length,  $r_c = 1$ . The different parts of the forces are given by the following Equations.

$$f_{ij}^C = \begin{cases} a_{ij}(1-r_{ij})e_{ij} & (r_{ij} < 1) \\ 0 & (r_{ij} \geq 1) \end{cases} \tag{3}$$

$$f_{ij}^D = -\gamma\omega^D(r_{ij})(v_{ij}e_{ij})e_{ij} \tag{4}$$

$$f_{ij}^R = \sigma\omega^R(r_{ij})\zeta_{ij}\Delta t^{-\frac{1}{2}}e_{ij} \tag{5}$$

where  $r_{ij} = r_i - r_j$ ,  $r_{ij} = |r_{ij}|$ ,  $e_{ij} = r_{ij}/r_{ij}$ , and  $v_{ij} = v_i - v_j$ .  $\zeta_{ij}$  is a random number with zero mean and unit variance.  $A_{ij}$  is a

constant which describes the maximum repulsion between interacting beads.  $\omega^D$  and  $\omega^R$  represent  $r$ -dependent weight functions for the dissipative and random forces, respectively, and vanish for  $r > r_c = 1$ .

The bead interactions ( $a_{ij}$ ) can be mapped through the  $\chi$ -parameter [25] as:

$$a_{ij} = a_{ii} + 3.27\chi_{ij} \tag{6}$$

$$\chi_{ij} = \frac{V_{ij}(\delta_i - \delta_j)^2}{RT} \tag{7}$$

where  $V_{ij}$  is the arithmetic average of molar volumes of beads  $i$  and  $j$ .  $\delta_i$  and  $\delta_j$  are the solubility parameters of beads  $i$  and  $j$ ,

**Table 2** The interaction parameters of PLA-PEG beads for 50/50 wt% PLA/PLA<sub>x</sub>-PEG<sub>y</sub>-PLA<sub>x</sub> blends. Two types of PLA were denoted as PLA<sub>H</sub> (PLA homopolymer) and PLA<sub>B</sub> (PLA block in copolymer)

	PLA <sub>B</sub>	PEG	PLA <sub>H</sub>
PLA/PLA <sub>3</sub> -PEG <sub>37</sub> -PLA <sub>3</sub>			
PLA <sub>B</sub>	25.00	30.79	25.00
PEG	30.79	25.00	28.17
PLA <sub>H</sub>	25.00	28.17	25.00
PLA/PLA <sub>12</sub> -PEG <sub>37</sub> -PLA <sub>12</sub>			
PLA <sub>B</sub>	25.00	29.94	25.00
PEG	29.94	25.00	28.17
PLA <sub>H</sub>	25.00	28.17	25.00
PLA/PLA <sub>27</sub> -PEG <sub>37</sub> -PLA <sub>27</sub>			
PLA <sub>B</sub>	25.00	28.17	25.00
PEG	28.17	25.00	28.17
PLA <sub>H</sub>	25.00	28.17	25.00

\*The numeric subscripts are denoted to number of DPD beads for PLA<sub>3</sub>-PEG<sub>37</sub>-PLA<sub>3</sub>, PLA<sub>12</sub>-PEG<sub>37</sub>-PLA<sub>12</sub>, and PLA<sub>27</sub>-PEG<sub>37</sub>-PLA<sub>27</sub> (equivalent to  $f_{PLA}$  = 0.126, 0.280, 0.469 respectively) corresponding to experimental studies

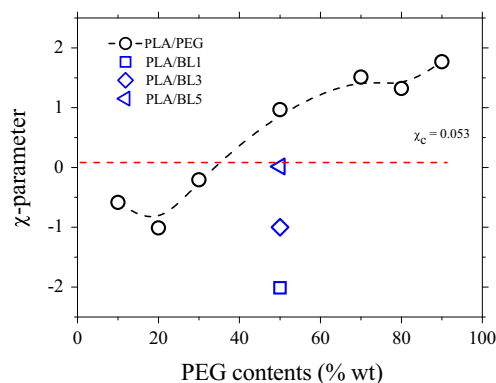


**Fig. 1** The calculated Flory-Huggins interaction ( $\chi$ ) parameter of PLA/PEG and PLA/PLA<sub>x</sub>-PEG<sub>y</sub>-PLA<sub>x</sub> blends (BL1, BL3 and BL5 are denoted as PLA<sub>3</sub>-PEG<sub>50</sub>-PLA<sub>3</sub>, PLA<sub>11</sub>-PEG<sub>50</sub>-PLA<sub>11</sub> and PLA<sub>25</sub>-PEG<sub>50</sub>-PLA<sub>25</sub>, respectively)

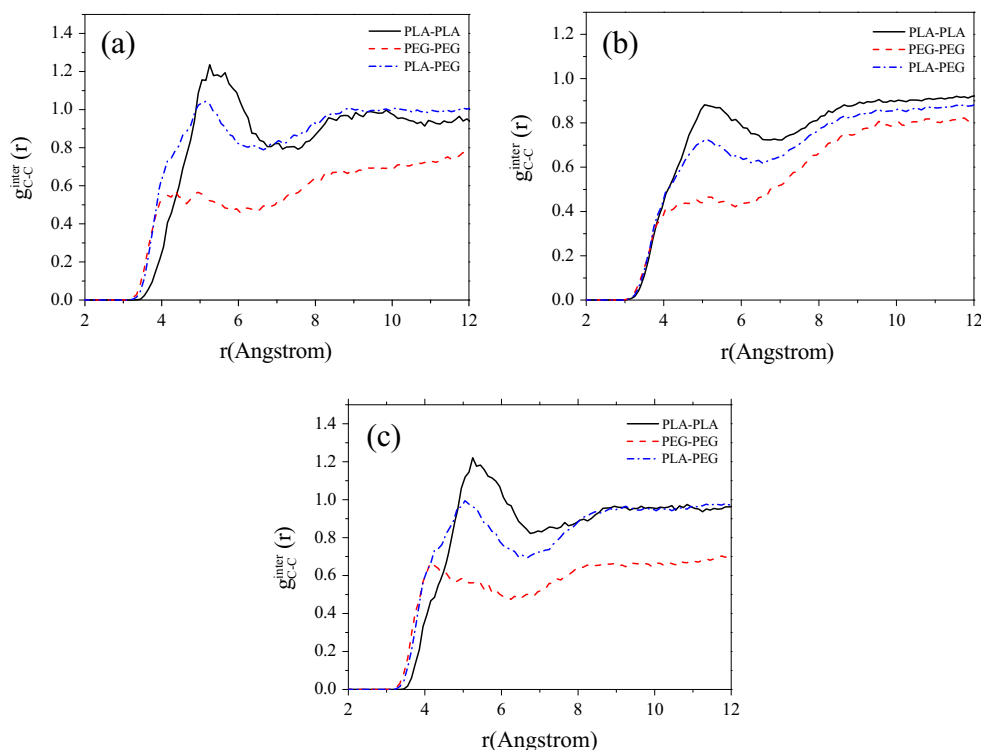
respectively, which were depend on the chemical nature of each species. The interaction parameter between the same type beads  $a_{ii}$  equals 25. The procedure for calculating  $\chi_{ij}$  parameter is described in MD simulation section. This  $\chi_{ij}$  parameter is put into the Eq. (7), for the interaction in DPD simulation.

DPD simulations of the mixtures of PLA/PEG and PLA/PLA<sub>x</sub>-PEG<sub>y</sub>-PLA<sub>x</sub> were performed with a bead density ( $\rho$ ) of 3. The influence of the simulation box sizes (from  $20 \times 20 \times 20$  to  $50 \times 50 \times 50$ ) was also investigated but there was no apparent finite size effect for the box size of  $30 \times 30 \times 30$  or bigger. Therefore, DPD was performed in a

cubic box of size  $30 \times 30 \times 30$  with 3D periodic boundary conditions. The simulations were performed at reduced temperature ( $k_B T$ ) = 1, which allows a reasonable and efficient relaxation for each binary blend. A total of  $10^5$  time steps with step size ( $\Delta t$ ) = 0.05 in DPD reduced units were performed for equilibration.

PLA, PEG and PLA<sub>x</sub>-PEG<sub>y</sub>-PLA<sub>x</sub> block copolymers with the molecular weight of 100,000, 8000 and 9440–125,936 g/mol which correspond to experimental studies were used. The number of DPD beads ( $N_{DPD}$ ) for PLA, PEG and PLA<sub>x</sub>-PEG<sub>y</sub>-PLA<sub>x</sub> were considered from the molar mass of polymers, molar mass of repeat units, degree of polymerization and the characteristic ratio as described in Eq. (1). One DPD bead is equivalent to 3 PLA or 5 PEG repeating units. For PLA/PEG blends, number of DPD beads per chain for PLA = 408 and PEG = 37. For PLA/PLA<sub>x</sub>-PEG<sub>y</sub>-PLA<sub>x</sub> blends, PLA<sub>3</sub>-PEG<sub>37</sub>-PLA<sub>3</sub>, PLA<sub>12</sub>-PEG<sub>37</sub>-PLA<sub>12</sub>, and PLA<sub>27</sub>-PEG<sub>37</sub>-PLA<sub>27</sub> (subscripts here at PLA and PEG are the number of DPD beads), with different PLA block fraction ( $f_{PLA} = 0.126, 0.280, 0.479$  closed to 0.107, 0.306, 0.500 for BL1, BL3 and BL5, respectively, used in previous MD simulation) were selected to blend with PLA homopolymer. The composition of PLA in PLA<sub>x</sub>-PEG<sub>y</sub>-PLA<sub>x</sub> blend was set at 50 wt% with respect to PEG content. The Gaussian chain models and the bead-bead pair interactions parameters  $a_{PLA-PEG}$  for PLA/PLA<sub>x</sub>-PEG<sub>y</sub>-PLA<sub>x</sub> blends are presented in Table 2. The interaction between PLA and PEG beads in PLA/PLA<sub>x</sub>-PEG<sub>y</sub>-PLA<sub>x</sub> blends can be divided into two kinds

**Fig. 2** Radial distribution functions,  $g(r)$  of the inter-molecular carbon-carbon pairs for 50/50 wt% of (a) PLA/PLA<sub>3</sub>-PEG<sub>50</sub>-PLA<sub>3</sub> (b) PLA/PLA<sub>11</sub>-PEG<sub>50</sub>-PLA<sub>11</sub> and (c) PLA/PLA<sub>25</sub>-PEG<sub>50</sub>-PLA<sub>25</sub>



i.e. (1) the intrachain PLA-PEG bead interaction within the block copolymer and (2) the interaction between PLA homopolymer and PEG block in copolymer. The magnitude for each interaction is depended on PLA and PEG composition.

## Experiment

### Materials

The commercial grade PLA (PLA2002D, Nature Work) was used as polymer host for preparing the PLA/PEG and PLA/PLA<sub>x</sub>-PEG<sub>y</sub>-PLA<sub>x</sub> blends and PEG (8000 g/mol) was used as the reference plasticizer [17] and also used for preparing block copolymers. Triblock copolymers of lactide (3, 6-Dimethyl-1, 4-dioxane-2, 5-dione, D, L-lactide) and PEG (8000 g/mol) were synthesized via ring opening polymerization using Sn(Oct)<sub>2</sub> as the catalyst (all chemicals from Aldrich). To prevent crystallization of PLA block, D, L-lactide (DLLA), were used to synthesize PLA<sub>x</sub>-PEG<sub>y</sub>-PLA<sub>x</sub> with various PLA block fractions ( $f_{PLA}$ ). Molecular weights of these block copolymers were controlled by varying the ratio of DLLA monomer to PEG polymer. Block copolymers of PLA<sub>36</sub>-PEG<sub>187</sub>-PLA<sub>36</sub>, PLA<sub>72</sub>-PEG<sub>187</sub>-PLA<sub>72</sub> and PLA<sub>87</sub>-PEG<sub>187</sub>-PLA<sub>87</sub> were synthesized. All blends were prepared by solution mixing methods using dichloromethane as the solvent.

### Characterization

Proton Nuclear Magnetic Resonance (<sup>1</sup>H-NMR) spectrometry (JEOL instrument) was used to determine the structure and molecular characteristics of the synthesized block copolymers. Molecular weight ( $\bar{M}_w$  and  $\bar{M}_n$ ) and molecular weight distribution (MWD) were determined using Shimadzu LC 20A gel permeation chromatography equipped with the reflective index detector (RID-10A). A PLgel 5 mm MIXED-D column, with a guard column was used. The eluent used was tetrahydrofuran (THF). Calibration was accomplished using polystyrene (PS) standards with molecular weight = 451,000, 186,000, 42,900 and 6390 g/mol. Differential Scanning Calorimeter (DSC) thermograms of polymers were recorded on Pyris Diamond (Perkin-Elmer) with nitrogen as the purge gas. An indium standard was used for the calibration. The viscoelastic properties of polymers were measured using Anton Parr MCR300 rheometer, equipped with parallel plate geometry (8 mm  $\phi$ ). To compare with the data for PLA/PEG in the previous study at the terminal region, measurements are carried out at 180 °C. Linear viscoelastic region was determined by performing an amplitude sweep and then frequency sweep measurements are performed.

## Results and discussion

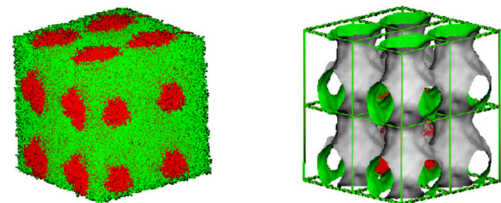
### MD simulation

#### Flory-Huggins parameters

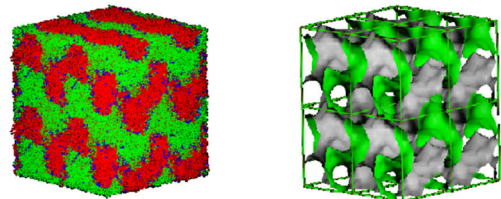
Miscibility of polymer blends can be predicted using examining the Flory-Huggins parameter ( $\chi_{AB}$ ) defined as

$$\chi_{AB} = \left( \frac{\Delta E_{mix}}{RT} \right) V_m \quad (8)$$

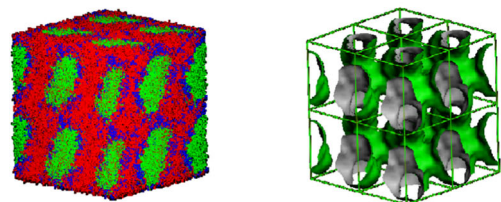
where  $V_m$  is the molar volume of the repeating unit chosen as a reference (57.7 cm<sup>3</sup>/mol for PLA),  $R$  is the molar gas constant and  $T$  is the temperature in Kelvin. The energy of mixing,  $\Delta E_{mix}$  can be calculated by



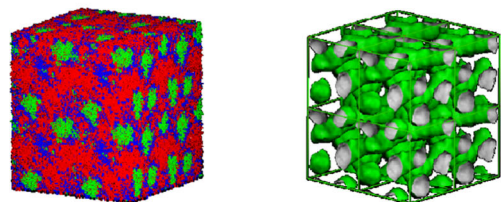
(a) PLA/PEGa



(b) PLA/PLA<sub>3</sub>-PEG<sub>37</sub>-PLA<sub>3</sub>



(c) PLA/PLA<sub>12</sub>-PEG<sub>37</sub>-PLA<sub>12</sub>



(d) PLA/PLA<sub>27</sub>-PEG<sub>37</sub>-PLA<sub>27</sub>

**Fig. 3** Morphologies (left) and iso-density surfaces of PEG segment (right) of 50/50 (wt/wt) PLA/PEG and PLA/PLA<sub>x</sub>-PEG<sub>y</sub>-PLA<sub>x</sub> blends from DPD simulation

$$\Delta E_{mix} = \phi_A \left( \frac{E_{coh}}{V} \right)_A + \phi_B \left( \frac{E_{coh}}{V} \right)_B - \phi_{mix} \left( \frac{E_{coh}}{V} \right)_{mix} \quad (9)$$

where the terms in parenthesis represent the cohesive energies ( $E_{coh}/V$ ) of pure polymers (A and B) and the blend (mix),  $\phi_A$  and  $\phi_B$  represent volume fractions of polymers in the blend,  $\phi_A + \phi_B = 1$ .

A positive  $\chi_{AB}$  should indicate immiscibility for blends of high molecular weight polymers. In addition, one can compare  $\chi_{AB}$  with the critical  $\chi$ -parameter ( $\chi_c$ ) to predict the blend miscibility.

$$\chi_c = \frac{1}{2} \left( \frac{1}{\sqrt{n_A}} - \frac{1}{\sqrt{n_B}} \right)^2 \quad (10)$$

where  $n_A$  and  $n_B$  are the degrees of polymerization of pure polymers. If  $\chi_{AB} < \chi_c$ , the blend is miscible. If  $\chi_{AB}$  is slightly larger than  $\chi_c$ , the blend exhibits partial miscibility. For larger  $\chi_{AB}$ , it should be completely immiscible.

Figure 1 presents the variation of  $\chi$  versus PEG weight fraction for PLA/PEG and PLA/PLA<sub>x</sub>-PEG<sub>y</sub>-PLA<sub>x</sub> blends. The MD-calculated  $\chi$  was increased from  $-1.01$  to  $1.77$  for PLA/PEG blends. For 90/10, 80/20 and 70/30 wt% PLA/PEG blends,  $\chi_{PLA-PEG}$  is clearly below  $\chi_c$  line, indicating miscibility only at these compositions. It is apparent that the  $\chi$ -parameters of 50/50 wt% PLA/PLA<sub>x</sub>-PEG<sub>y</sub>-PLA<sub>x</sub> blends are always lower than those of PLA/PEG blends and these  $\chi$ -parameters

are also well below the  $\chi_c$  line. Thus, miscibility was enhanced by blending with PLA<sub>x</sub>-PEG<sub>y</sub>-PLA<sub>x</sub> block copolymer. The higher PLA block fraction, the better miscibility.

#### Radial distribution function

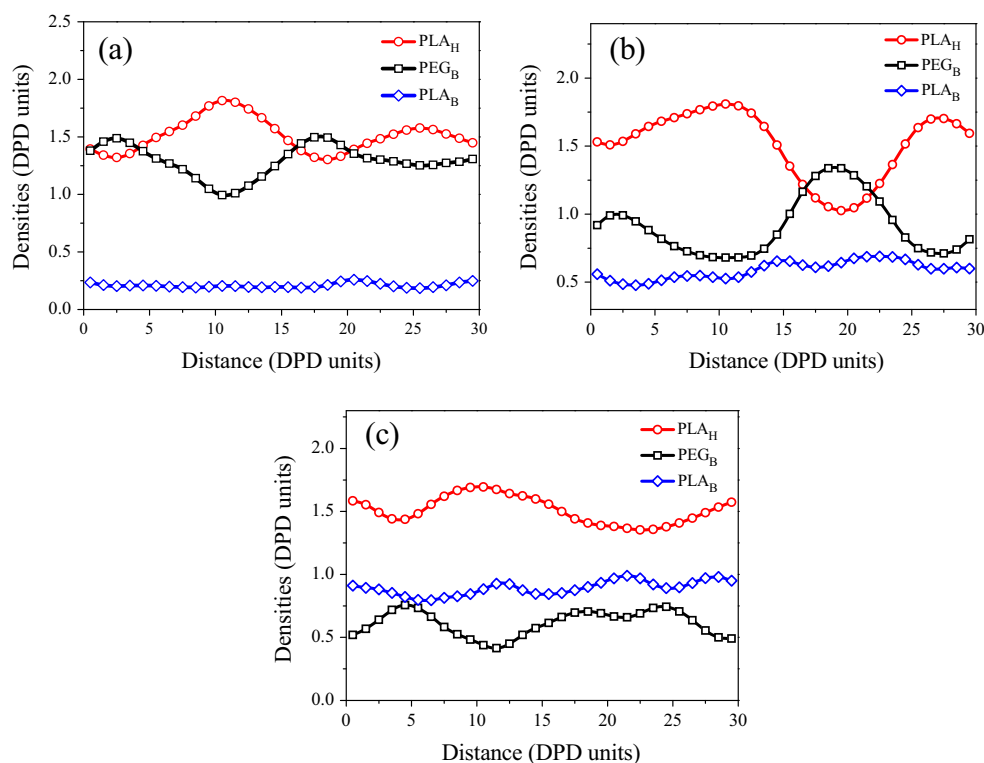
Radial distribution function  $g(r)$  is commonly used to characterize the molecular structure which gives the probability of finding a particle at the distance  $r$  from another particle. It can be defined as:

$$g_{AB}(r) = \frac{1}{\rho_{AB} 4\pi r^2 \delta r} \frac{\sum_{i=1}^k \sum_{j=1}^{N_{AB}} \Delta N_{AB}(r \rightarrow r + \delta r)}{N_{AB} k} \quad (11)$$

where  $N_{AB}$  is the total number of atoms of A and B in the system,  $k$  is the number of time steps,  $\delta r$  is the distance interval,  $\Delta N_{AB}$  is the number of B (or A) atoms between  $r$  to  $r + \delta r$  around an A (or B) atom and  $\rho_{AB}$  is the bulk density. If a binary system is miscible, the intermolecular  $g(r)$  of A-B pairs between two different polymers is larger than those of AA and BB pairs.

For 50/50 wt% PLA/PLA<sub>x</sub>-PEG<sub>y</sub>-PLA<sub>x</sub> blends,  $g(r)$  for the carbon atomic pairs of PLA-PLA, PEG-PEG and PEG-PLA are presented in Fig. 2a–c. As expected,  $g(r)$  of PLA-PLA are higher than those of PEG-PEG and PLA-PEG for all systems indicating that PLA chains prefer to interact with PLA rather

**Fig. 4** Density profiles of (a) PLA/PLA<sub>3</sub>-PEG<sub>37</sub>-PLA<sub>3</sub>, (b) PLA/PLA<sub>12</sub>-PEG<sub>37</sub>-PLA<sub>12</sub> and (c) PLA/PLA<sub>27</sub>-PEG<sub>37</sub>-PLA<sub>27</sub> blends calculated by DPD simulation



than PEG. Interestingly,  $g(r)$  of PEG-PEG is always lower than that of PLA-PEG for all PLA/PLA<sub>x</sub>-PEG<sub>y</sub>-PLA<sub>x</sub> blends. This phenomenon points toward better dispersion of PEG segments in PLA matrix.

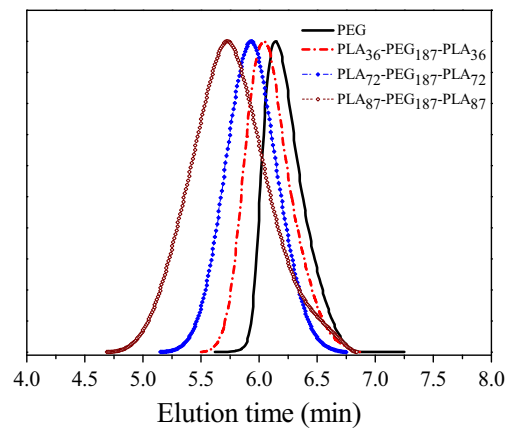
**DPD simulation**

Figure 3 shows DPD results for the morphologies and iso-density surfaces of PEG component (fixed at 50 wt% composition), for PLA/PEG, PLA/PLA<sub>3</sub>-PEG<sub>37</sub>-PLA<sub>3</sub>, PLA/PLA<sub>12</sub>-PEG<sub>37</sub>-PLA<sub>12</sub> and PLA/PLA<sub>27</sub>-PEG<sub>37</sub>-PLA<sub>27</sub> (here, subscripts at PLA and PEG are the number of DPD units) The bicontinuous-like structures of PEG domain observed in PLA/PLA<sub>3</sub>-PEG<sub>37</sub>-PLA<sub>3</sub> and PLA/PLA<sub>12</sub>-PEG<sub>37</sub>-PLA<sub>12</sub> are gradually change to rod/spherical-like structures in PLA/PLA<sub>27</sub>-PEG<sub>37</sub>-PLA<sub>27</sub>. The size reduction of PEG domain is because the aggregated PEG components tend to break up and PLA<sub>x</sub>-PEG<sub>y</sub>-PLA<sub>x</sub> can be more disperses in the PLA matrix. The density profiles of PLA homopolymer (PLA<sub>H</sub>), PEG and PLA components of PLA<sub>x</sub>-PEG<sub>y</sub>-PLA<sub>x</sub> (PEG<sub>B</sub>, PLA<sub>B</sub>) in the blends are displayed in Fig. 4. It is seen that PLA segments in block copolymer are located at the interface between PLA homopolymer and PEG components. This indicates that PEG segments can be distributed more in PLA phase contributed to PLA end blocks. Figure 4a–c also show the bead density profiles of PLA<sub>H</sub>, PEG<sub>B</sub> and PLA<sub>B</sub> in PLA/PLA<sub>x</sub>-PEG<sub>y</sub>-PLA<sub>x</sub> blends. Apparently, the density profiles of each species in PLA/PLA<sub>x</sub>-PEG<sub>y</sub>-PLA<sub>x</sub> exhibit the characteristics of phase separation. In contrast, the density profiles of PLA<sub>H</sub>, PEG<sub>B</sub> and PLA<sub>B</sub> in PLA/PLA<sub>27</sub>-PEG<sub>37</sub>-PLA<sub>27</sub> are relatively constant, in different from other blends, indicating that PLA<sub>27</sub>-PEG<sub>37</sub>-PLA<sub>27</sub> can be most dispersed in PLA matrix. In addition, the magnitude of  $\chi_{PLA_B-PEG_B}$  is very close to  $\chi_{PLA_H-PEG_B}$  in PLA/PLA<sub>27</sub>-PEG<sub>37</sub>-PLA<sub>27</sub>, suggesting that PEG component is preferably more dispersed into the PLA matrix.

**Table 3** Characteristics of PEG, PLA, and PLA<sub>x</sub>-PEG<sub>y</sub>-PLA<sub>x</sub> with different block composition and PLA stereochemistry

Sample	<sup>1</sup> H-NMR			GPC		$f_{PLA}$
	LA/EG	$DP_{(PLA)}$	$M_n$	$M_n$	$M_w/M_n$	
PEG	–	–	–	8.23	1.24	–
PLA2002D (PLA)	–	–	–	58.32	3.32	1
PLA <sub>36</sub> -PEG <sub>187</sub> -PLA <sub>36</sub>	0.38	36	13.42	11.38	1.35	0.28
PLA <sub>72</sub> -PEG <sub>187</sub> -PLA <sub>72</sub>	0.78	72	18.62	17.13	1.45	0.44
PLA <sub>87</sub> -PEG <sub>187</sub> -PLA <sub>87</sub>	0.93	87	20.78	21.81	2.36	0.48

$\overline{DP}$  of PEG = 187.  $f_{PLA}$  is calculated from <sup>1</sup>H-NMR and  $\overline{M}_n$  is represented in kg/mol



**Fig. 5** GPC chromatograms of PLA<sub>36</sub>-PEG<sub>187</sub>-PLA<sub>36</sub>, PLA<sub>72</sub>-PEG<sub>187</sub>-PLA<sub>72</sub> and PLA<sub>87</sub>-PEG<sub>187</sub>-PLA<sub>87</sub>

**Characterization**

*Nuclear magnetic resonance*

There are three main group of peaks in <sup>1</sup>H-NMR spectra of PLA<sub>x</sub>-PEG<sub>y</sub>-PLA<sub>x</sub> (Figure not shown here). The peak at  $\delta \approx 4.37$  ppm is the  $\alpha$ -methylene protons of PLA block connecting to EG units (PLA-COO-CH<sub>2</sub>-), together with CH protons of the hydroxylated lactyl end units. Resonances in the range of 5.20–5.14 ppm (–CH) and 1.5–1.4 ppm (–CH<sub>3</sub>) are belonged to PLA blocks. Signal at  $\delta \approx 3.6$  ppm is the characteristics of main chain methylene units within PEG blocks. The signals of carboxylated lactyl end units and free lactide of which methine protons should appear in the 5.0–4.9 ppm and at 4.03 ppm are not observed indicating that homo-polymerization of lactide is neglectable at this condition [26, 27].

<sup>1</sup>H-NMR technique was also utilized to evaluate molecular weight ( $\overline{M}_n$ ) of block copolymer using the relationship in Eqs. (12) and (13).

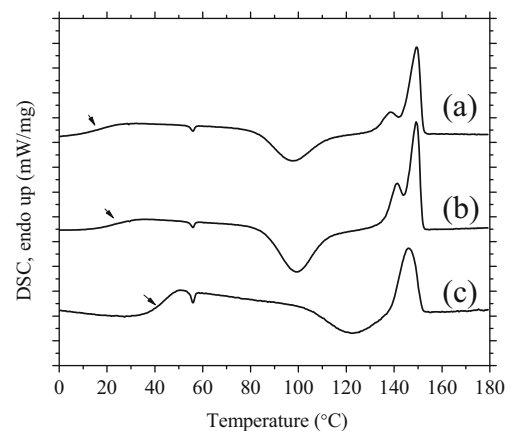


**Fig. 6** Subsequent heating DSC thermograms of (a) PLA/PLA<sub>36</sub>-PEG<sub>187</sub>-PLA<sub>36</sub>, (b) PLA/PLA<sub>72</sub>-PEG<sub>187</sub>-PLA<sub>72</sub> and (c) PLA/PLA<sub>87</sub>-PEG<sub>187</sub>-PLA<sub>87</sub> obtained with a heating rate of 10 °C/min. The PEG content in the blends is 30 wt%. Arrows indicate the position of  $T_g$

$$\overline{M}_{n(\text{PLA-PEG-PLA})} = \overline{M}_{n(\text{PEG})} + 2\overline{M}_{n(\text{PLA})} + 18 \quad (12)$$

where  $\overline{M}_{n(\text{PLA})}$  can be calculated as:

$$\overline{M}_{n(\text{PLA})} = \frac{\overline{DP}_{(\text{PEG})}x(\text{LA}/\text{EG})}{2} \quad (13)$$

The mole ratio of LA and EG in block copolymer can be deduced from integration of NMR resonances of PLA ( $\delta \approx 5.20$  ppm) and PEG blocks ( $\delta \approx 3.65$  ppm) [27]. The characteristics of synthesized copolymer are summarized in Table 3.

#### Gel permeation chromatography

Figure 5 depicts chromatograms of PEG and  $\text{PLA}_x\text{-PEG}_y\text{-PLA}_x$  with various composition for each PLA stereochemistry. From these chromatograms, single peak was observed for each sample and the peak shift indicates that block copolymers were effectively obtained. However, since the lower molecular weight edges of chromatograms are overlapped so that we cannot neglect the existence of residual PEG and/or PLA homopolymer from GPC analysis alone. Together with the NMR results, we can safely assume that residual PEG and/or PLA homopolymer are negligible and do not affect the results in this study. Molecular weight and molecular weight distributions determined from these GPC results are presented in Table 3.

#### Thermal characterization of $\text{PLA}/\text{PLA}_x\text{-PEG}_y\text{-PLA}_x$ blends

Figure 6 shows the subsequent second heating DSC thermograms of  $\text{PLA}/\text{PLA}_{36}\text{-PEG}_{187}\text{-PLA}_{36}$  to  $\text{PLA}/\text{PLA}_{87}$ -

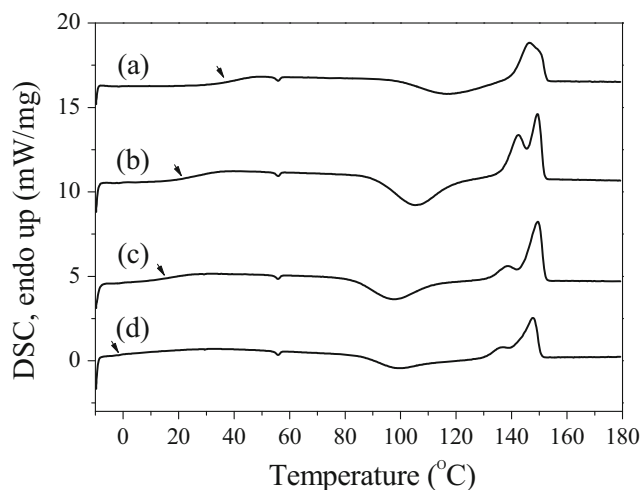


**Fig. 7** Subsequent heating DSC thermograms of quenched  $\text{PLA}/\text{PLA}_{72}\text{-PEG}_{187}\text{-PLA}_{72}$  with different compositions (a) 90/10 wt/wt, (b) 80/20 wt/wt, (c) 70/30 wt/wt and (d) 50/50 wt/wt obtained with a heating rate of  $10^\circ\text{C}/\text{min}$ . Arrows indicate the position of  $T_g$

$\text{PEG}_{187}\text{-PLA}_{87}$  blends. It is clear that there is no endothermic melting peak of PEG component in all these blends (see Fig. 5 in ref. [17]). An increased  $T_g$  for LA component is observed for  $\text{PLA}/\text{PLA}_{87}\text{-PEG}_{187}\text{-PLA}_{87}$  blend while  $\text{PLA}/\text{PLA}_{36}\text{-PEG}_{187}\text{-PLA}_{36}$  and  $\text{PLA}/\text{PLA}_{72}\text{-PEG}_{187}\text{-PLA}_{72}$  exhibit lower  $T_g$ . To further investigate the influence of copolymer content on thermal properties of the blends,  $\text{PLA}_{72}\text{-PEG}_{187}\text{-PLA}_{72}$  was chosen for further studies. DSC thermograms of  $\text{PLA}/\text{PLA}_{72}\text{-PEG}_{187}\text{-PLA}_{72}$  with different blend composition (10, 20, 30 and 50 wt% of  $\text{PLA}_{72}\text{-PEG}_{187}\text{-PLA}_{72}$  content) are presented in Fig. 7. The enthalpies change ( $\Delta H$ ) of cold crystallization and subsequent melting suggest that the quenched  $\text{PLA}/\text{PLA}_{72}\text{-PEG}_{187}\text{-PLA}_{72}$  are amorphous similar to  $\text{PLA}/\text{PEG}$  blends. Both cold crystallization and glass transition

**Table 4** Thermal properties of  $\text{PLA}/\text{PLA}_x\text{-PEG}_y\text{-PLA}_x$  blends at a heating rate of  $10^\circ\text{C}/\text{min}$

Sample	$T_g$ ( $^\circ\text{C}$ )	Cold crystallization			Melting			
		$T_c$ ( $^\circ\text{C}$ )	$\Delta H_c$ (J/g)	$X_{cc}$ (%)	$T_m$ ( $^\circ\text{C}$ )		$\Delta H$ (J/g)	$X_c$ (%)
					PEG	PLA**		
PLA	51.8	–	–	–	–	149.8	0.47	0.50
PEG	–	–	–	–	–	66.7	–	–
PLLA/B01 70:30	22.8	99.0	–30.0	32.1	–	141.4(149.2)	35.8	38.2
PLLA/B02 70:30	15.3	97.5	–23.1	24.7	–	138.4(149.7)	27.2	29.1
PLLA/B03 70:30	43.6	122.1	–10.9	11.6	–	146.3	10.3	11.0
PLLA/B02 90:10	41.6	116.5	–18.7	20.0	–	146.4	19.5	20.8
PLLA/B02 80:20	26.8	105.3	–33.2	35.5	–	142.2(149.4)	33.0	35.3
PLLA/B02 70:30	16.7	97.5	–24.2	25.9	–	138.4(149.4)	26.6	28.4
PLLA/B0250:50	–0.29	99.2	–32.0	34.2	–	136.0(147.6)	40.1	42.8

\*All PLA are denoted to PLLA2002D

\*\*xxx.x(yyy.y) refer to the first and second  $T_m$  peaks of PLA

\*\*\*Symbols of B01, B02 and B03 are denoted as  $\text{PLA}_{36}\text{-PEG}_{187}\text{-PLA}_{36}$ ,  $\text{PLA}_{72}\text{-PEG}_{187}\text{-PLA}_{72}$  and  $\text{PLA}_{87}\text{-PEG}_{187}\text{-PLA}_{87}$ , respectively



temperature are decreased for higher PEG content in the blends. Furthermore, the crystallinity of PLA is increased as shown in Table 4. PLA/PLA<sub>72</sub>-PEG<sub>187</sub>-PLA<sub>72</sub> blend exhibits only a single  $T_g$  implying that B02 is miscible with PLA. Figure 8 shows that, at the same PEG composition,  $T_g$  of PLA/PLA<sub>72</sub>-PEG<sub>187</sub>-PLA<sub>72</sub> is always higher than PLA/PEG blends. This may seem that PEG is better plasticizer than PLA<sub>72</sub>-PEG<sub>187</sub>-PLA<sub>72</sub>; however, PLA/PEG at 50:50 wt% actually exhibits phase separation [17]. In addition to  $T_g$  criteria, the melting point depression can also be used as an indicator for miscibility of the blends containing crystallizable components. Figure 9 illustrates the melting temperature ( $T_m$ ) of PLA in the blends as a function of PEG content. Compared to PLA/PEG,  $T_m$  of PLA component in PLA/PLA<sub>72</sub>-PEG<sub>187</sub>-PLA<sub>72</sub> is apparently lower implying that PLA<sub>72</sub>-PEG<sub>187</sub>-PLA<sub>72</sub> should hinder PLA crystallization better than PEG. This is typical characteristics for miscible blends composed of an amorphous and crystallizable polymers.

*Rheological characterization*

The corresponding  $G'$  and  $G''$  for these blends are shown in Fig. 10. As expected, Both  $G'$  and  $G''$  are decreased for higher plasticizer concentration. All polymer samples exhibit the rheological behavior of typical polymer melts ( $G' < G''$ ), though the frequency dependence of  $G'$  is slightly lower than 2. All samples show common frequency dependence for dynamic moduli except for  $G'$  of 30 wt% PLA<sub>72</sub>-PEG<sub>187</sub>-PLA<sub>72</sub> at lower frequency region, where the elastic modulus significantly deviates from the slope close to 2. The elastic modulus enhancement was reported in many studies for immiscible polymer blends [28, 29] and it is generally attributed to the shape change of the discrete phase in polymer matrix during an oscillatory shear deformation, namely shape relaxation (Ferry, 1980). On the other hand, the loss moduli of all blends did not show sign of shape relaxation.

The deviation of  $G'$  data from the terminal region behavior for 30 wt% PLA<sub>72</sub>-PEG<sub>187</sub>-PLA<sub>72</sub> is similar to those observed

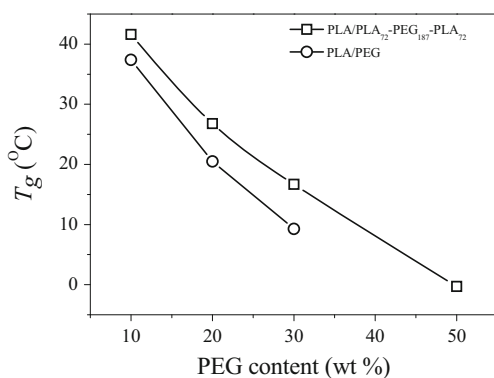


**Fig. 8** Glass transition temperature ( $T_g$ ) of PLA/PLA<sub>72</sub>-PEG<sub>187</sub>-PLA<sub>72</sub> and PLA/PEG blends [17] as a function of PEG content

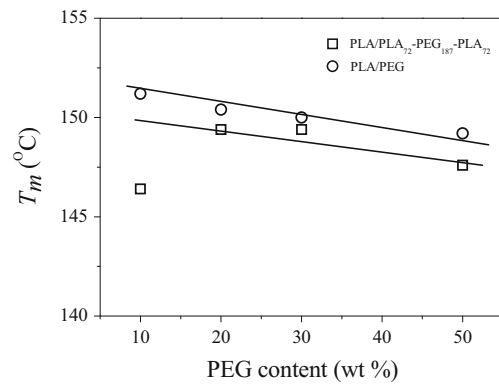


**Fig. 9** Melting temperature ( $T_m$ ) of PLA/PLA<sub>72</sub>-PEG<sub>187</sub>-PLA<sub>72</sub> and PLA/PEG blends [17] as a function of PEG content

for PLA/PEG (PEG content of 25 and 30%) blends at the low frequency region in the previous work. As already discussed in [17], such behavior of  $G'$  can be attributed to either phase separation or strong concentration fluctuation near the phase separation point. Compared with the same PEG content blend, we can conclude that PLA<sub>72</sub>-PEG<sub>187</sub>-PLA<sub>72</sub> is less contributed to phase separation than PEG plasticizer, indicating that PLA<sub>72</sub>-PEG<sub>187</sub>-PLA<sub>72</sub> is better miscible with PLA.

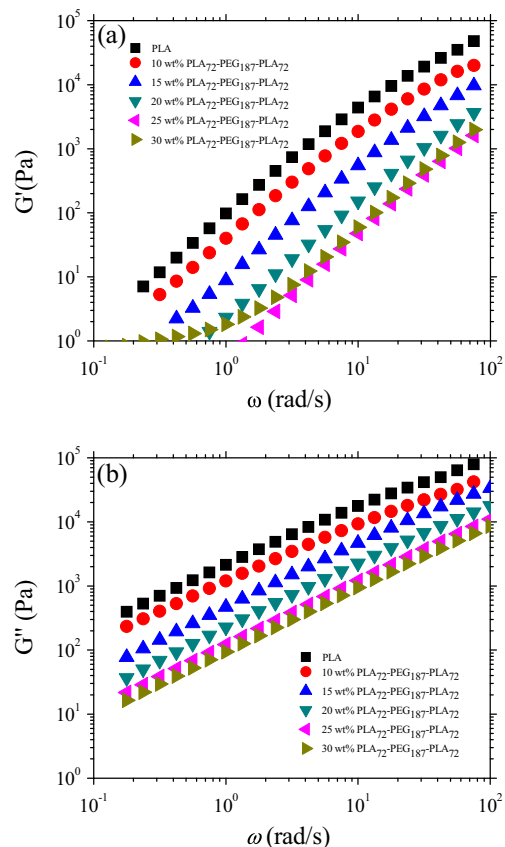


**Fig. 10** Frequency ( $\omega$ ) dependencies of (a) storage modulus ( $G'$ ) and (b) loss modulus ( $G''$ ) of PLA/PLA<sub>72</sub>-PEG<sub>187</sub>-PLA<sub>72</sub> with different PLA<sub>72</sub>-PEG<sub>187</sub>-PLA<sub>72</sub> contents at 180 °C

## Conclusion

Atomistic and mesoscale simulations were employed to predict the miscibility and morphology of PLA/PLA<sub>x</sub>-PEG<sub>y</sub>-PLA<sub>x</sub> blends. For PLA/PLA<sub>x</sub>-PEG<sub>y</sub>-PLA<sub>x</sub> with PLA block fractions = 0.1–0.5,  $\chi_{ij}$ -parameters of PLA and PEG for all PLA/PLA<sub>x</sub>-PEG<sub>y</sub>-PLA<sub>x</sub> are lower than those of PLA/PEG blends.  $X_{ij}$  of PLA/PLA<sub>x</sub>-PEG<sub>y</sub>-PLA<sub>x</sub> is decreased for higher PLA block fractions. The radial distribution functions of intermolecular carbon atomic pairs of PLA-PEG, PLA-PLA and PEG-PEG also indicate that PLA/PLA<sub>x</sub>-PEG<sub>y</sub>-PLA<sub>x</sub> is better miscible. Based on mesoscale simulation, the PEG domain in PLA/PLA<sub>x</sub>-PEG<sub>y</sub>-PLA<sub>x</sub> blends is smaller than that in PLA/PEG blend. This implies that the PLA end blocks should contribute to miscibility enhancement. Experimental results based on thermal and rheological analysis also confirm better miscibility for PLA/PLA<sub>x</sub>-PEG<sub>y</sub>-PLA<sub>x</sub> compared to PLA/PEG blends in consistent with the prediction by molecular simulation.

**Acknowledgements** The financial support for A.T. by the Commission on Higher Education, Ministry of Education (Thailand) for supporting the grant fund under the program Strategic Scholarships for Frontier Research Network for the Ph.D. Program is gratefully acknowledged. All molecular simulation works were done at Suranaree University of Technology (SUT), Thailand, and most of the experimental part was performed at Kyushu University, Japan. A.T. and V.V. would like to thank National Nanotechnology Center, Thailand, for their permission to use Material Studio software.

## References

- Auras R, Lim LT, Selke SEM, Tsuji H (2010) Poly(lactic acid): synthesis, structures, properties, processing and applications. Wiley, Canada
- Garlotta D (2001) A literature review of poly(lactic acid). *J Polym Environ* 2(9):63–84
- Lui H, Zhang J (2011) Research progress in toughening modification of poly(lactic acid). *J Polym Sci B Polym Phys* 15:1051–1083
- Sheth M, Kumar RA, Dave V, Gross RA, McCarthy SP (1997) Biodegradable polymer blends of poly(lactic acid) and poly(ethylene glycol). *J Appl Polym Sci* 66:1495–1505
- Lemmouchi Y, Murariu M, Margarida Dos Santos A, Amass AJ, Schacht E, Dubois P (2009) Plasticization of poly(lactide) with blends of tributyl citrate and low molecular weight poly(D,L-lactide)-b-poly(ethylene glycol) copolymers. *Eur Polym J* 45: 2839–2848
- Rathi S, Chen X, Coughlin EB, Hsu SL, Golub CS, Tzivanis MJ (2011) Toughening semicrystalline poly(lactic acid) by morphology alteration. *Polymer* 52:4181–4188
- Hu Y, Hu YS, Topolkarav V, Hiltner A, Baer E (2003) Crystallization and phase separation in blends of high stereoregular poly(lactide) with poly(ethylene glycol). *Polymer* 44:5681–5689
- Hu Y, Rogunova M, Topolkarav V, Hiltner A, Baer E (2003) Aging of poly(lactide)/poly(ethylene glycol) blends: Part 1. Poly(lactide) with low stereoregularity. *Polymer* 44:5701–5710
- Hamley IW (1998) The physics of block copolymer. Oxford University Press, New York
- Nakafuku C, Takehisa SY (2004) Glass transition and mechanical properties of PLLA and PDLLA-PGA copolymer blends. *J Appl Polym Sci* 93:2164–2173
- Anderson KS, Lim SH, Hillmyer MA (2002) Toughening of polylactide by melt blending with linear low-density polyethylene. *J Appl Polym Sci* 89:3757–3768
- Jia Z, Tan J, Han C, Yang Y, Dong L (2009) Poly(ethylene glycol-co-propylene glycol) as a macromolecular plasticizing agent for polylactide: Thermomechanical properties and aging. *J Appl Polym Sci* 114:1105–1117
- Hansen KK, Neilson CJ, Hvilsted S (2004) Low molecular weights block copolymers as plasticizers for polystyrene. *J Appl Polym Sci* 95:981–991
- Spyriouni T, Vergelati C (2001) Molecular modeling study of binary blend compatibility of polyamide 6 and poly(vinyl acetate) with different degrees of Hydrolysis: an atomistic and mesoscopic approach. *Macromolecules* 34:5306–5316
- Yang H, Sheng LZ, Qian HJ, Yang YB, Zhang XB, Sun CC (2004) Molecular dynamics simulation studies of the miscibility of poly(3-hydroxybutyrate) and poly(ethylene oxide). *Polymer* 45: 453–457
- Glotzer SC, Paul W (2002) Molecular and mesoscale simulation methods for polymer materials. *Annu Rev Mater Res* 32:401–436
- Takhulee A, Takahashi Y, Vao-soongnern V (2017) Molecular simulation and experimental studies of the miscibility of polylactic acid/polyethylene glycol blends. *J Polym Res* 24:8
- Flory PJ (1989) Statistical mechanics of chain molecules. Hanser, Germany
- Theodorou DN, Suter UW (1986) Atomistic modeling of mechanical properties of polymeric glasses. *Macromolecules* 19:139–154
- Meirovitch H (1983) Computer simulation of self-avoiding walks: testing the scanning method. *J Chem Phys* 79:502
- Mu D, Huang XR, ZY L, Sun CC (2008) Computer simulation study on the compatibility of poly(ethylene oxide)/poly(methyl methacrylate) blends. *Chem Phys* 348:122–129
- Jawalkar SS, Aminabhavi TM (2006) Molecular modeling simulations and thermodynamic approaches to investigate compatibility/incompatibility of poly(L-lactide) and poly(vinyl alcohol) blends. *Polymer* 47:8061–8071
- Sun H (1998) COMPASS: an Ab initio forcefield optimized for condensed-phase application-overview with details on alkane and benzene compounds. *J Phys Chem B* 102:7338–7364
- Hoogerbrugge PJ, Koelman JMVA (1992) Simulating microscopic hydrodynamic phenomena with dissipative particle dynamics. *Europhys Lett* 19:155–160
- Groot RD, Warren PB (1997) Dissipative particle dynamics: bridging the gap between atomistic and mesoscopic simulation. *The Journal of Chemical Physical* 107:4423–4435
- Du YJ, Lemstra PJ, Nijenhuis AJ, Aert HAMV, Bastiaansen C (1995) ABA type copolymers of lactide with poly(ethylene glycol): Kinetic, mechanistic, and model studies. *Macromolecules* 28: 2124–2132
- Rashkov I, Manolova N, Li SM, Espartero JL, Vert M (1996) Synthesis, characterization, and hydrolytic degradation of PLA/PEO/PLA triblock copolymer with short poly(L-lactic acid) chains. *Macromolecules* 20:50–56
- Noroozi N, Schafer LL, Hatzikiriakos SG (2012) Thermorheological properties of poly( $\epsilon$ -caprolactone)/polylactide blends. *Polym Eng Sci* 52:2348–2359
- Gu SY, Zhang K, Ren J, Zhan H (2008) Melt rheology of polylactide/ poly(butylene adipate-co-terephthalate) blends. *Carbohydr Polym* 74:79–85